

Low Profile/Single Layer X-Band Circularly Polarized Reflectarray with a Linearly Polarized Feed

Shimaa A. M. Soliman^{1, 2, *}, Ahmed M. Attiya¹, and Yahia M. Antar³

Abstract—This paper presents a design of a right hand circularly polarized x-band reflectarray antenna (RA) at a center frequency 12 GHz. The reflectarray is fed by a linearly polarized dipole antenna. The proposed reflectarray antenna can be used for CubeSat applications. The reflecting elements have the shape of a pentagon. This shape is chosen to convert the incident linearly polarized fields to the required circular polarization. A dipole antenna is used as linearly polarized (LP) feeding element for the proposed reflectarray. This dipole antenna is tilted w.r.t the x -axis by an angle 45° to introduce nearly equal polarizations in x and y directions on the aperture of the reflectarray. Each reflecting element is adjusted to produce a phase shift 90° between the reflection coefficients in x and y directions. The required reflected phase is realized by adjusting a scaling factor (SF) for the pentagonal patch in x direction to the corresponding SF in y axis. This phase difference is responsible for polarization conversion of the incident plane wave into circularly polarized reflected wave. The reflectarray is designed with focal to-diameter (F/D) ratio equals unity. In this work, an efficient technique is discussed for modelling the reflectarray designed. This technique is based on developing a Visual Basic Script file for allocating the reflecting elements with their corresponding dimensions in their location on the simulation tool. This script file is used directly by the simulation tool (HFSS) to draw the complete model automatically. This procedure has a significant role on simplifying the modeling of complicated structure like the proposed reflectarray. The proposed reflectarray antenna is simulated at 12 GHz. The obtained axial ratio (AR) is found to be 2.1 dB, and peak gain is 18 dBi. The antenna is also fabricated and measured for verification.

1. INTRODUCTION

CubeSats are small satellites, light weight and low cost which provide access to space with possibilities to realize Internet of Space (IoS), and aim to provide global network access, especially for remote areas. Due to the small size, there are a limited volume in the spacecraft to mount the antenna systems required for remote sensing applications and data transmission links [1–3]. The establishment of a high-data-rate communication link between a CubeSat and the Earth requires a planar and high-gain antenna.

A reflectarray antenna consists of a planar array of reflecting elements which are illuminated by a feeding antenna, in a similar way to a parabolic reflector antenna. To generate a collimated or a shaped beam, the reflecting elements are designed to introduce the required phase distribution on aperture of the reflectarray [4, 5]. Linear-to-circular polarization conversion can also be obtained by adjusting the geometry of the reflecting element. Various reflectarrays have been proposed to achieve linear polarizations (LP) by using reflecting elements with the required phase of reflection over a wide frequency range [6, 7]. However, in many applications, circular polarization (CP) may be preferred to

Received 1 July 2022, Accepted 29 August 2022, Scheduled 11 September 2022

* Corresponding author: Shimaa Ahmed Megahed Soliman (shimaa_megahed@eri.sci.eg).

¹ Microwave Engineering Department, Electronics Research Institute (ERI), Cairo, Egypt. ² Department of Electrical and Computer Engineering, Queen's University, Kingston, ON, Canada. ³ Department of Electrical and Computer Engineering, Royal Military College of Canada, Kingston, ON, Canada.

reduce losses caused by multipath fading, Faraday rotation, and polarization mismatch [8]. The design of CP reflectarrays is considered a challenging task. Several CP reflectarrays have been designed with remarkable performance in terms of gain, power, bandwidth, cross-polarization levels, and axial ratio (AR) [9, 10].

A CP reflectarray can be obtained by two different methods. The first one is by using a CP feeding source with a reflectarray composed of angularly rotated reflecting elements to obtain the phase delay for the CP reflectarrays [11, 12]. The second method is by applying an LP feed to illuminate the reflectarray elements which convert the incident linearly polarized field into circularly polarized fields [13, 14]. In this case, the reflecting elements are designed to transform LP incident waves into CP reflected waves and to collimate the resulting radiated fields in the far field. Different shapes of reflecting elements were used to design CP reflectarrays with an LP feed [15–17]. On the other hand, horn antenna is usually used as an LP feed for reflectarray. However, in this paper, a dipole antenna is used as the feeding antenna for the proposed reflectarray to reduce the blockage effect of the feeding element. This dipole antenna also has the advantages of less weight and lower profile than a standard horn antenna [18, 19]. In this paper, a new design of a CP reflectarray composed of pentagon-shaped patches reflecting elements illuminated by an LP dipole antenna is proposed. The proposed CP reflectarray covers the satellite communication which operates at the X-band at frequency 12 GHz. The flat surface of the RA simplifies the mounting of the antenna on a small spacecraft.

Figure 1 shows the geometry of the proposed reflectarray antenna. It consists of a reflectarray centered at the origin at the x - y plane. The reflectarray is composed of pentagonal reflecting elements printed on a grounded dielectric substrate. This reflectarray is fed by a dipole antenna which is located at the focal point along the z axis. The dipole antenna is parallel to the x - y plane, and it is tilted by an angle 45° w.r.t the x -axis. This orientation introduces nearly equal field components in x and y directions on the aperture of the reflectarray. On the other hand, by controlling a scaling factor of reflecting pentagonal patches in x direction, it would be possible to adjust the phase distribution of the reflected waves in x direction to introduce the required radiation pattern of the reflectarray. Moreover, by adjusting the aspect ratio of the scaling factor (SF) for the pentagon in x direction to the corresponding SF in y axis, it would be possible to adjust the phase shift between the reflection coefficient in x direction and the reflection coefficient in y direction to be 90° . Thus, by adjusting the

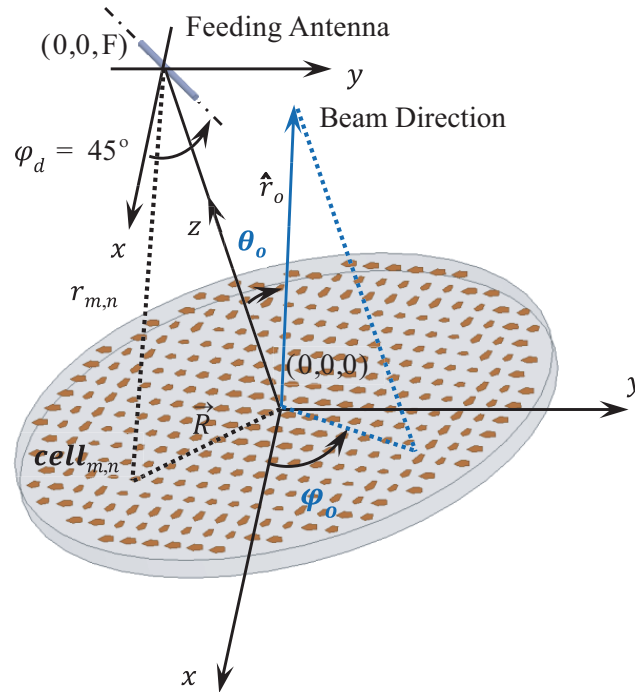


Figure 1. Geometry of the proposed reflectarray antenna.

phase shift between the x and y components of the reflected fields, it would be possible to convert the linearly polarized incident plane wave of the feeding dipole antenna to a collimated circularly polarized radiation pattern from the reflectarray.

This paper is organized as follows. Section 2 discusses the design of the pentagon reflecting element. Section 3 presents the design of the complete structure of the CP reflectarray with an LP feeding dipole antenna. Section 4 presents the automation method for modeling the layout of the proposed reflectarray. Section 5 presents the results and discussions. The concluding remarks are presented in Section 6.

2. ANALYSIS AND DESIGN OF THE SINGLE ELEMENT

The reflecting element has a pentagon-shaped patch. The advantage of this pentagon shape is that it enables circular polarization through excitation of orthogonal modes in the introduced cavity under the patch. This pentagon shape was used before in designing circularly polarized microstrip patch antenna [20]. However, up to our best knowledge, it was not used before as a reflecting element in reflectarray antenna. Figure 2(a) shows the geometry of the reflecting element. The dimensions of the unit cell are $dx \times dy$. For the case of circularly polarized patch antenna, the required conditions to introduce circular polarization are $b/a = 1.0603$, $c/a = 0.3061$ [20]. The reflectarray elements are arranged in a rectangular cell. The periodicity of this unit cell is chosen to be half the free space wavelength at the center operating frequency $f_0 = 12$ GHz. Thus, the periodicity in x - y plane is $d_x = d_y = 12.5$ mm. Hence, the maximum allowable value for the length of the reflecting element is chosen to be $a = 12$ mm. The remaining dimensions of the reflecting patch are obtained in terms of the length a . The reflecting elements are printed on a grounded FR4 substrate with a dielectric constant $\epsilon_r = 4.4$ and a dielectric thickness $h = 1.5$ mm.

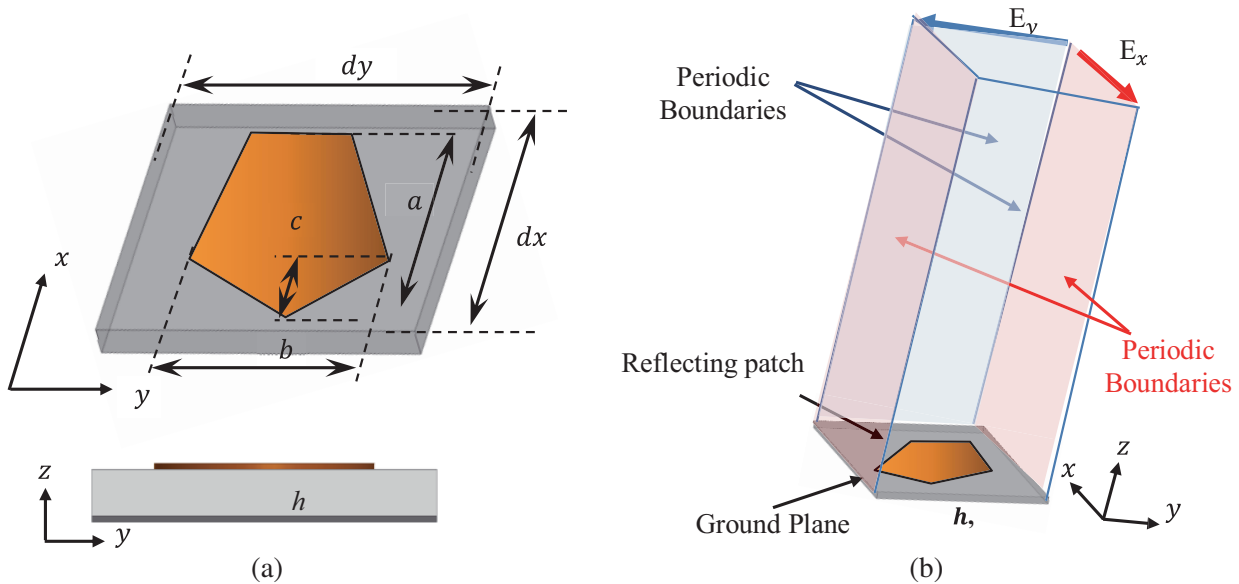


Figure 2. (a) Geometry of the pentagon patch reflecting element. (b) Simulation model of a reflecting element inside periodic boundary conditions.

The phase of the reflected fields from a reflecting element is obtained by simulating the reflecting element in periodic boundaries to model an infinite periodic structure. The model of the reflecting element unit cell inside periodic boundary conditions is shown in Figure 2(b). A Floquet port with a normal incident wave is used to excite the LP incident plane wave for both x - and y -polarizations. The reflection coefficients of these two orthogonal LP incident waves can be controlled to generate reflected CP plane waves by adjusting the scaling factor of the pentagon in x and y directions.

Figure 3 shows the phase of the reflection coefficient as a function of the SF at the center frequency f_0 . It can be noted that the phase of the reflected field can be controlled over a range from 0° to 320°

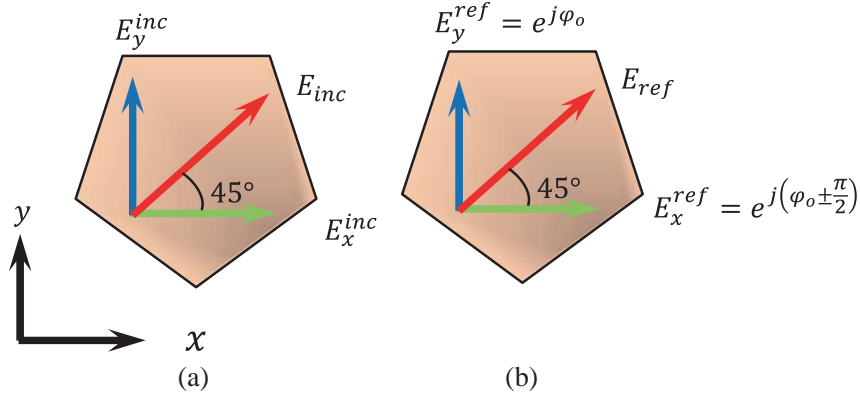


Figure 3. (a) Decomposition of the incident LP at 45° slant into two orthogonal components in the direction of the x and y . (b) Decomposition of the reflected wave in the direction of the x and y .

corresponding to SF ranging from 0.3 to 0.8 which is considered a suitable and wide range of phase for obtaining the required phase distribution. Whereas, the pentagonal patch is characterized by its two scaling factors SF_x and SF_y , in x and y directions, respectively. To convert an incident linearly polarized wave to a circularly polarized wave, the incident polarization should be tilted by an angle $\pi/4$ w.r.t the x axis to obtain two equal linearly polarized components in x and y directions on the plane of the reflectarray as shown in Figure 3. In addition, it is required to maintain the phase shift between the reflection coefficients of these two components to be $\pi/2$ to obtain circular polarization. Thus, from Figure 4, a single point is chosen where the phase difference between the phases of the reflection coefficients of the x polarized and the y polarized components is $\pi/2$. This procedure is repeated for different values of the SF_y in the y direction to obtain the corresponding value of SF_x in the x direction which satisfies this condition. Then, a lookup table is generated for the phase of the reflection coefficient of the y polarized wave as a function of the value of SF_y and the corresponding value of SF_x which introduce a phase shift $\pi/2$ in the reflection coefficient of the x polarized wave.

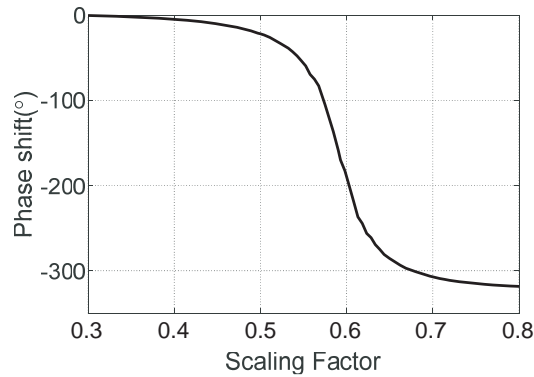


Figure 4. Phase of the reflection coefficient of the reflected signal from the reflecting element in periodic boundaries as a function of the scaling factor.

3. DESIGN OF THE REFLECTARRAY ANTENNA STRUCTURE

The CP reflectarray antenna is designed by using the proposed pentagonal reflecting element presented earlier in Section 2. The structure is composed of an array of reflecting elements organized on planar circular disk in front of an LP dipole antenna. The diameter of the reflectarray is 26.25 cm which is equivalent to $10.5\lambda_0$ at the center frequency 12 GHz. The reflectarray is designed with a focal to diameter ratio (F/D) equals unity. The reflectarray is fed at its focal point by a $\lambda_0/2$ dipole antenna

which radiates a linearly polarized field. The dipole is rotated 45° with respect to the x -axis to introduce nearly equal excitations in x and y polarizations at the plane of the reflectarray. The required phase distribution along the aperture of the reflectarray to achieve a simple broadside pencil beam can be obtained as:

$$\Delta\varphi_{m,n} = 2\pi N' - k \left(r_{m,n} - \vec{R} \cdot \hat{r}_o \right) \quad (1)$$

where $N' = 1, 2, 3, \dots, r_{(m,n)}$ is the distance from the dipole to the m, n reflecting element; \vec{R} is the position vector from each element to the center of the array $(0, 0, 0)$; and \hat{r}_o is the position vector in the direction of the main beam of the reflectarray. Figure 5 shows the required phase distribution of the reflected fields along the aperture of the RA to provide a broadside radiation in $\theta_o = 0^\circ$ and $\varphi_o = 0^\circ$ direction. This phase distribution is implemented by arranging the reflecting elements with the corresponding SF for each element according to the required phases of the reflected fields at the position of these elements.

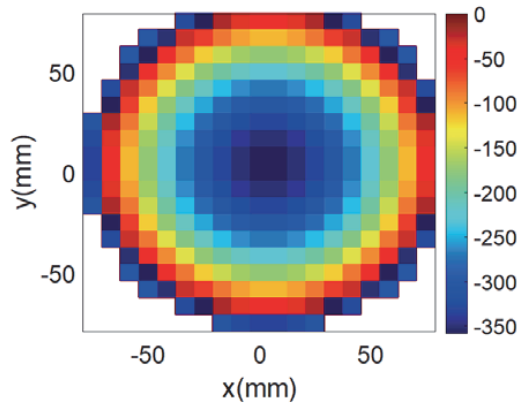


Figure 5. Phase distribution along the aperture of the reflectarray to provide a broadside radiation in $\theta_o = 0^\circ$ and $\varphi_o = 0^\circ$ direction.

4. AUTOMATION OF THE LAYOUT MODEL

To model the complete reflectarray assembly, it is required to allocate different reflecting elements in their positions according to the phase distribution shown in Figure 5. It should be noted that direct method for placing all reflecting elements with their corresponding dimensions in their locations would be quite complicated. One advantage of HFSS is that the geometry of the simulated structure can be presented by a Visual Basic Script (VBS), which can be loaded directly by HFSS to draw the required structure. This tool is quite useful for modeling complicated structures like the proposed reflectarray.

In the present case, we calculate the phase shift of the reflected fields for both x and y polarized fields as functions of the two scaling factors SF_x and SF_y as discussed in Section 2. By using these values, we generate a lookup table for different values of the phase shift ϕ_y in y direction as functions of SF_y and the corresponding values of SF_x which introduce simultaneous phase shift $\phi_x = \phi_y - 90^\circ$. Then we calculate the required phase distribution for the x polarized reflect fields from the aperture of the reflectarray as discussed in Section 3. According to this phase distribution and the center locations of the reflecting elements on the reflectarray, we determine the required values of SF_x and SF_y for each reflecting pentagonal patch on the aperture of the reflectarray. By using a loop algorithm, we can write the script line for drawing pentagon with a specific center location and scaling of its dimensions. The output of this loop algorithm would be the required Visual Basic Script which can be loaded by HFSS to draw the required reflectarray automatically.

This procedure presents a significant improvement in developing the model of the reflectarray. The array is built according to the following steps and simplified in the block diagram in Figure 6:

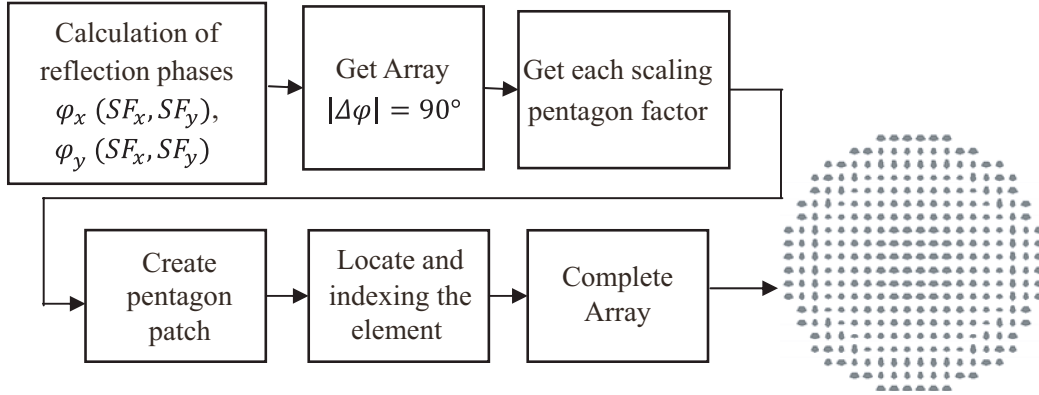


Figure 6. Block diagram for developing the simulation model of the reflectarray.

- Generate two dimensional arrays for $\varphi_x(SF_x, SF_y)$ and $\varphi_y(SF_x, SF_y)$ as a function of the two-dimensional parameters of the pentagon shape patch a and b.
- Achieving all array elements which satisfy that the phase difference $\Delta\varphi = |\varphi_x - \varphi_y| = 90^\circ$.
- Loop is executed using VBS for each element in an array, each element constructed with the dimensions of SF_x and SF_y , corresponding to the required phase distribution of the fields along the aperture of the RA to provide a broadside radiation.
- Naming and locating each elliptical patch from its center to its horizontal location on the aperture of the reflectarray.
- The reflectarray is ready to be simulated with the proposed feeding and the surrounding radiation boundaries.

5. RESULTS AND DISCUSSIONS

Figure 7 shows the layout of the designed reflectarray by using 316 pentagonal reflecting elements and the feeding dipole antenna at distance 262.5 mm and rotated by 45° with x -axis. Figure 8 shows the obtained 3D radiation pattern of the designed reflectarray at the center frequency 12 GHz. It has a broadside radiation with main beam in the direction $\theta_o = 0^\circ$ and peak gain 18.8 dB. Figure 9(a) and Figure 9(b) show the RHCP and LHCP components of this radiation pattern in the xz -plane ($\varphi_o = 0^\circ$) and ($\varphi_o = 90^\circ$), respectively. It can be noted that the designed array transmits RHCP wave. In Figure 10, the obtained axial ratio in the direction of the main beam is 2.1 dB. The cross-polarized

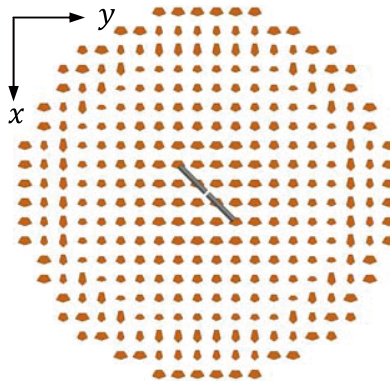


Figure 7. Layout of the proposed CP reflectarray antenna using the pentagon patches and the LP dipole antenna rotated 45° with x -axis.

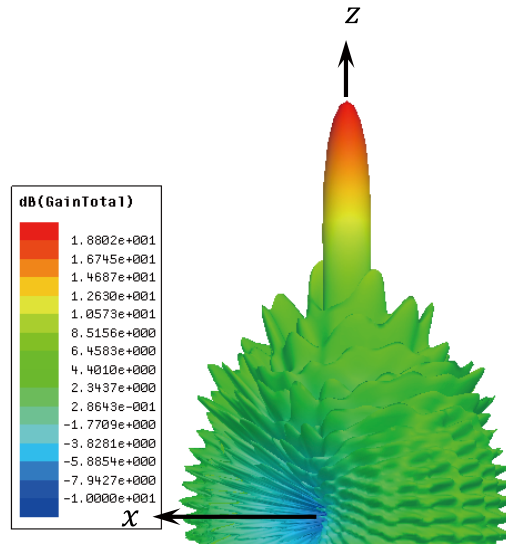


Figure 8. The simulated 3D radiation pattern of broadside pencil beam obtained by the proposed reflectarray antenna.

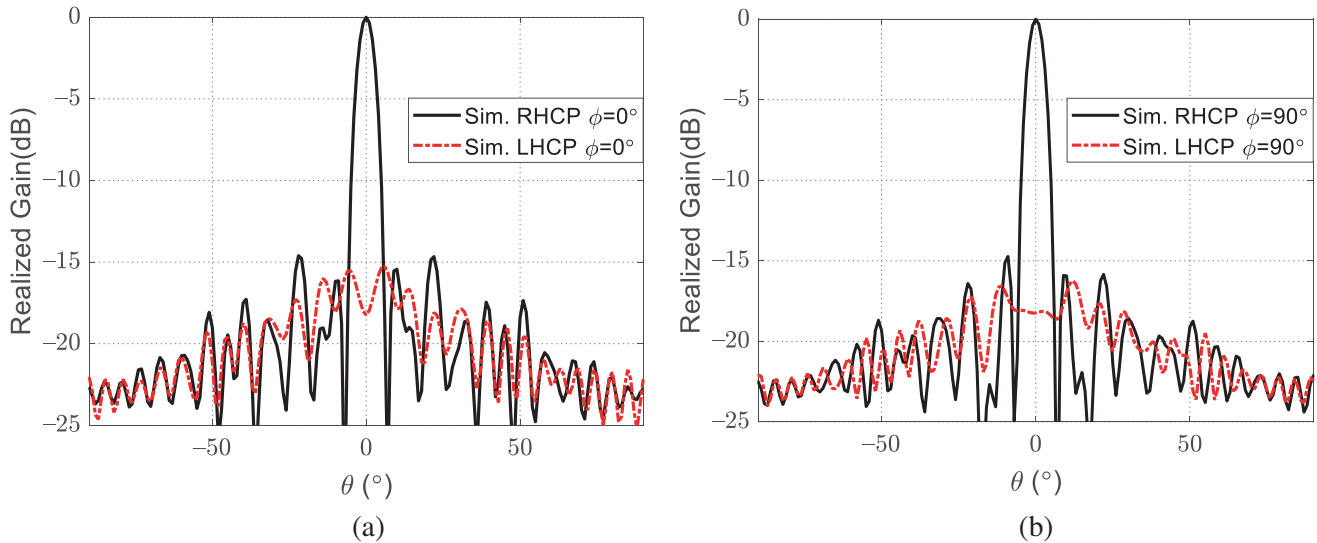


Figure 9. Plot of the simulated radiation pattern RHCP and LHCP at 12 GHz and in the xz -plane. (a) ($\varphi = 0^\circ$). (b) ($\varphi = 90^\circ$).

LHCP component is less than the co-polarized component by more than 15 dB in the direction of the main beam. The obtained results are quite suitable for the required application for the x-band satellite system.

For the sake of measuring the bandwidth performance of the proposed antenna array, it is simulated at two different frequencies ± 0.5 GHz. The results presented in Figure 11 show the broadside beam, the LHCP and RHCP components of the transmitted wave, at $\varphi = 0^\circ$ and $\varphi = 90^\circ$, and the axial ratio at two frequencies 11.5 GHz and 12.5 GHz. As noticed in the presented results, the antenna exhibits good performance with a wide bandwidth.

For verification the reflectarray antenna with a linearly polarized feeding is fabricated and measured. Figure 12 shows the measured $|S_{11}|$ for the feed antenna. It can be noted that $|S_{11}|$ at the required operating frequency 12 GHz is less than -20 dB. Figure 13 shows the fabricated reflectarray antenna with the feeding dipole antenna. The radiation pattern of the fabricated reflectarray antenna is measured as

shown in the setup in Figure 14. Figure 15 shows the measured normalized gain pattern in two different planes $\varphi = 0^\circ$ and $\varphi = 90^\circ$, respectively compared to the simulated results of the radiation with a peak gain 18 dBi. Figure 16 shows the measured and simulated cross polarization. The measured cross-

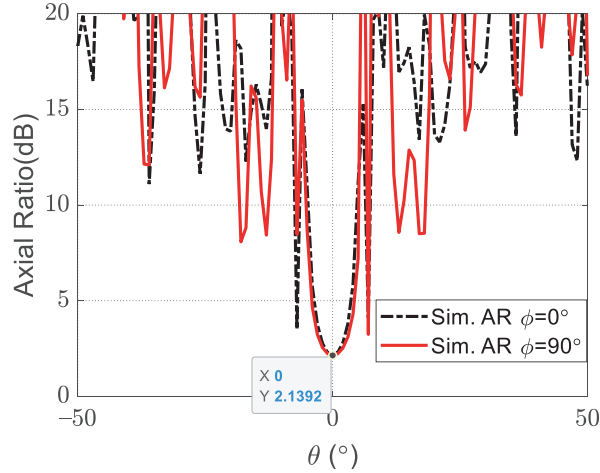
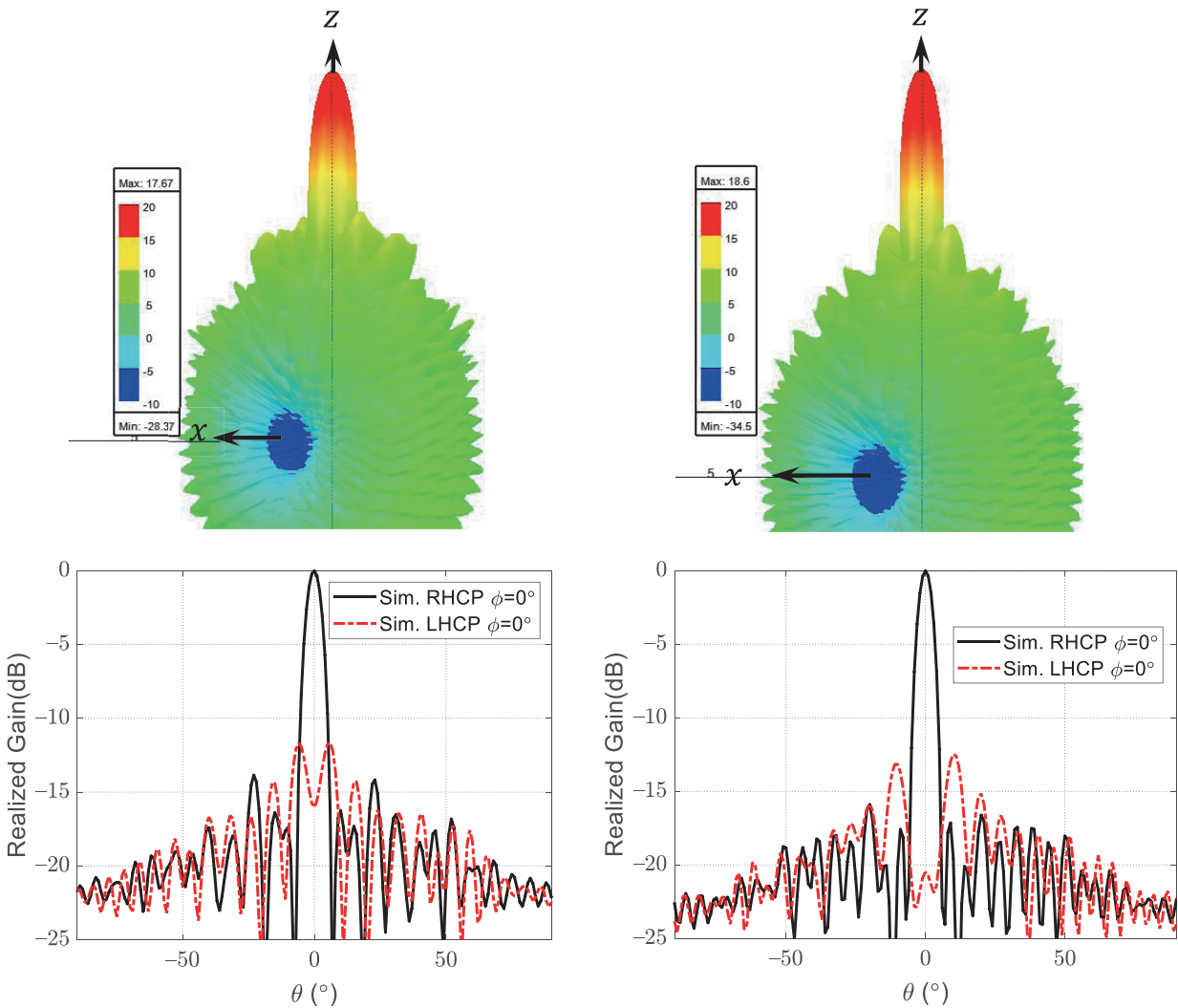


Figure 10. Plot of the simulated axial ratio at $\varphi = 0^\circ$ and $\varphi = 90^\circ$.



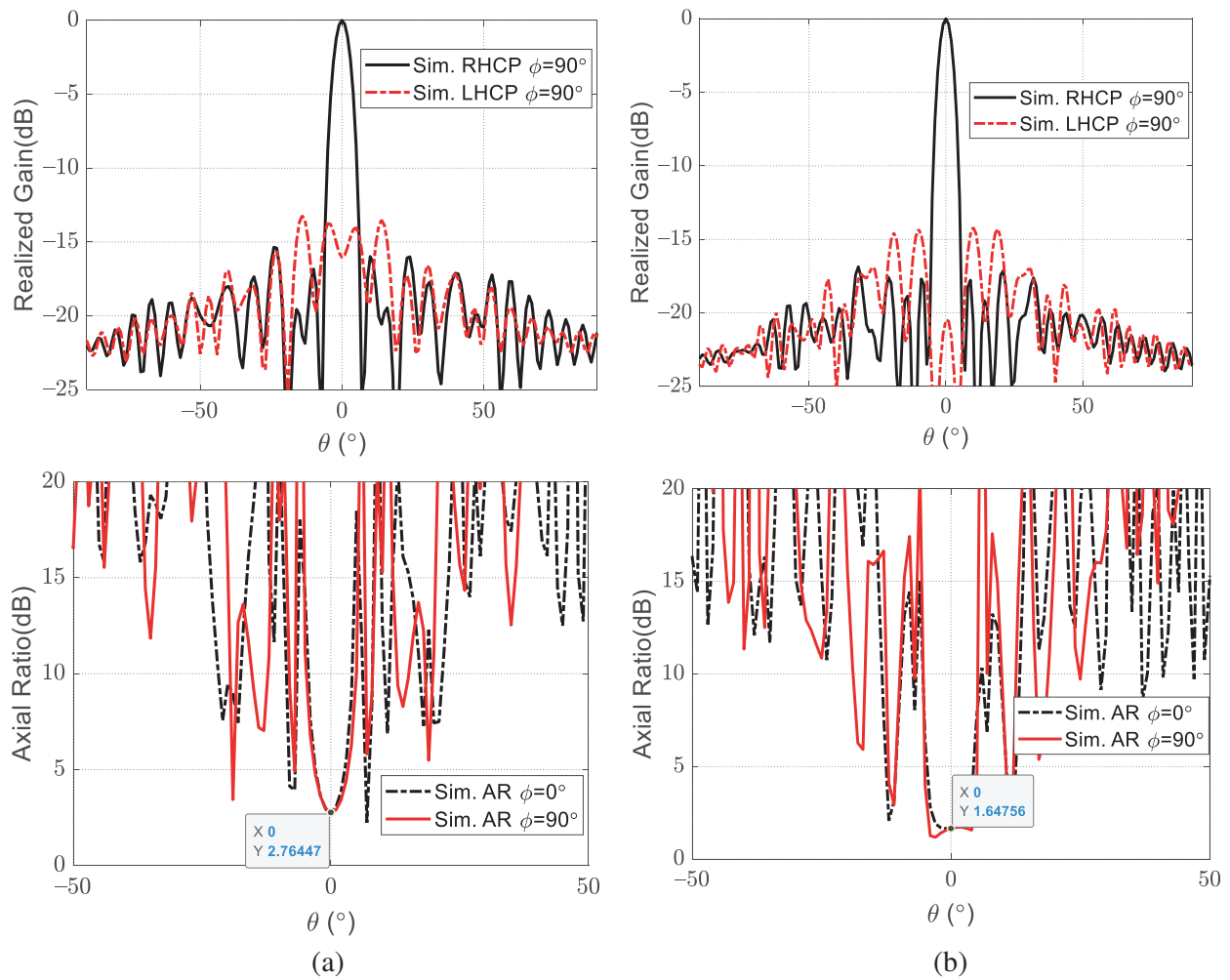


Figure 11. The radiation pattern, the LHCP and RHCP component, and the axial ratio at two frequencies. (a) 11.5 GHz and (b) 12.5 GHz.

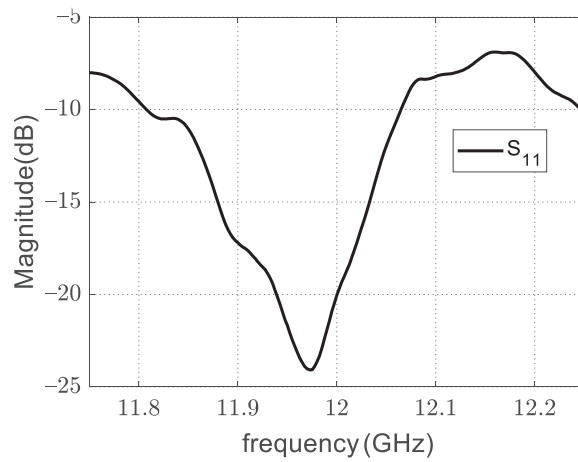


Figure 12. Variation of the measured magnitude of the reflection coefficient of the dipole antenna with frequency.

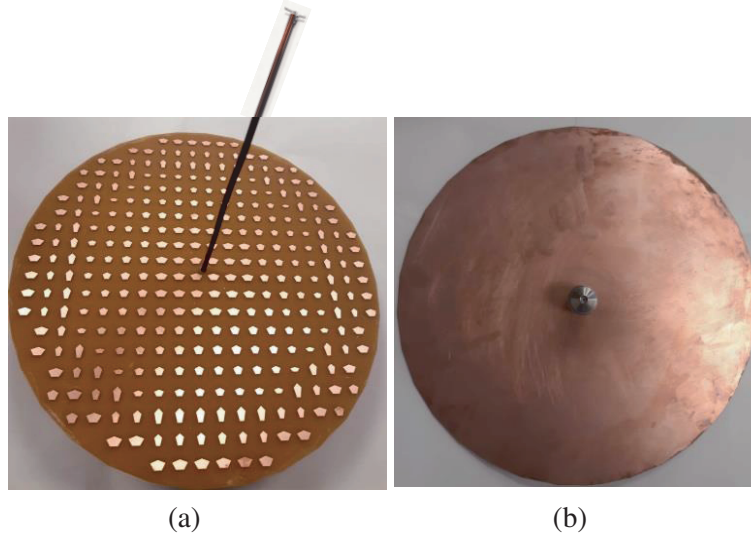


Figure 13. The fabricated prototype of the proposed reflectarray antenna with the feeding dipole antenna. (a) Top layer. (b) Bottom layer.

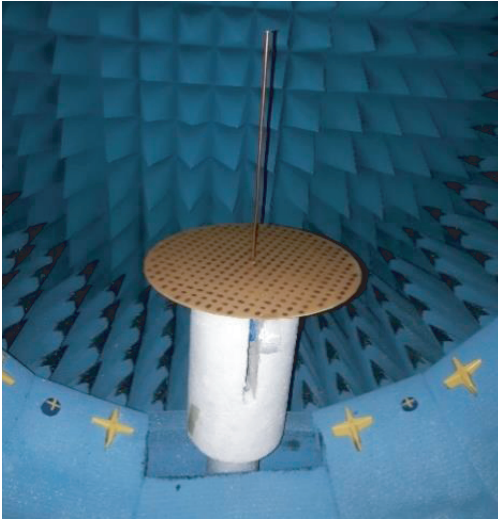


Figure 14. Fabricated reflectarray antenna inside the anechoic chamber for the radiation measurement.

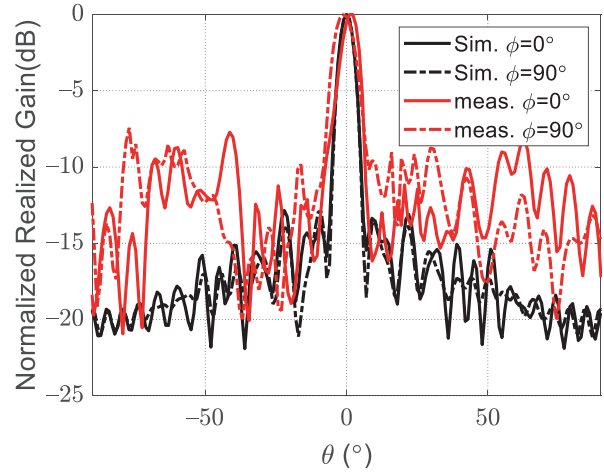


Figure 15. The measured radiation pattern of broadside pencil beam obtained by the proposed reflectarray antenna compared to the simulated results.

polarized LHCP component is less than the co-polarized component by more than 15 dB in the direction of the main beam. The difference between the measurement and simulation results can be explained due to the available measurement facility which is based on near field measurements with fixed dipole at discrete angles in azimuth direction. Then, the discretized near field measurements are converted to far field. In addition, the alignment and fixing procedure is done manually, which has some effect on the final measurements. Despite all these effects, the obtained measured results satisfy the required specifications. On the other hand, Figure 17 shows that the measured axial ratio in the direction of the main beam is 2.5 dB. Good agreements between the simulated and measured results can be noted. The simulated aperture efficiency is found to be 69.74% while the measured aperture efficiency is found to be 63.36%, which is quite acceptable. The aperture efficiency of the proposed antenna is quite low.

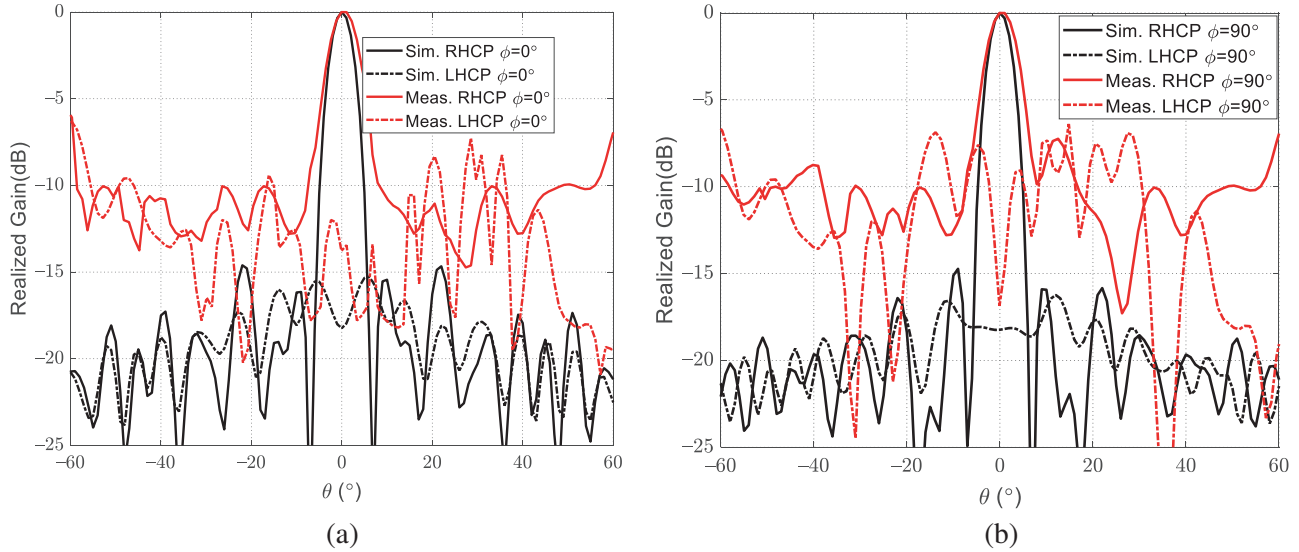


Figure 16. Plot of the measured and simulated radiation pattern RHCP and LHCP at 12 GHz and in the xz -plane. (a) ($\varphi = 0^\circ$). (b) ($\varphi = 90^\circ$).

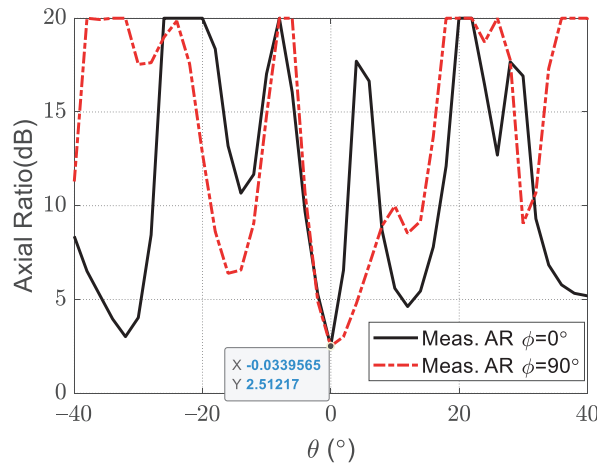


Figure 17. Plot of the measured axial ratio at $\varphi = 0^\circ$ and $\varphi = 90^\circ$.

The main reason for this is not the reflectarray but the feeding element. The simple dipole feeding element has a wide beam width, thus there is a lot of spill over. However, we preferred using dipole antenna instead of a standard horn antenna for two purposes: the first is to reduce the size and weight of the feeding element, and the second is to reduce the blockage effect. However, the main purpose of the present paper is to introduce an appropriate reflecting element for linear to circular polarization conversion.

6. CONCLUSION

A new design of single layer pentagonal shape reflecting element is used to construct an RA antenna to focus a high-gain beam at 12 GHz while converting the incident polarization from linear into circular polarization. This reflectarray antenna is suitable for small satellite applications. The proposed array consisting of 316 pentagonal reflecting elements arranged in circular aperture in two dimensions on planar surface with equal spacing equals $\lambda/2$ at the center frequency 12 GHz. The reflectarray is fed by a linearly polarized dipole antenna. Each reflecting element is adjusted to provide a 90°

phase difference between the reflection phases of the x and y polarizations to convert the linearly polarized wave into circularly polarized reflected wave. The complicated layout of the proposed model is developed automatically using VBS script. This procedure has a significant role in simplifying the simulation procedure. The designed reflectarray has an RHCP radiation with a peak gain 18.8 dBi, axial ratio 2.1 dB, and cross polarization level more than 15 dB at the center frequency 12 GHz. The proposed reflectarray was fabricated and measured for the verification of polarization conversion. The experimental results of the designed reflectarray are in good agreement with the simulation ones.

REFERENCES

1. Puig-Suari, J., C. Turner, and W. Ahlgren, "Development of the standard CubeSat deployer and a CubeSat class PicoSatellite," *Proceedings of the 2001 IEEE Aerospace Conference*, 1/347–1/353, Big Sky, MT, USA, Mar. 10–17, 2001.
2. Chahat, N., E. Decrossas, D. Gonzalez-Ovejero, O. Yurduseven, M. J. Radway, R. E. Hodges, P. Estabrook, J. D. Baker, D. J. Bell, T. A. Cwik, et al., "Advanced CubeSat antennas for Deep Space and Earth Science missions: A review," *IEEE Antennas Propag. Mag.*, Vol. 61, 37–46, 2019.
3. Bulgasem, S., F. Tubbal, R. Raad, P. I. Theoharis, S. Lu, and S. Iranmanesh, "Antenna designs for CubeSats: A review," *IEEE Access*, Vol. 9, 45289–45324J, 2021.
4. Huang, J. and J. A. Encinar, *Reflectarray Antennas*, Wiley/IEEE Press, Hoboken, NJ, USA, Nov. 2007, ISBN: 978-0-470-08491-5.
5. Shaker, J., M. R. Chaharmir, and J. Ethier, *Reflectarray Antennas: Analysis, Design, Fabrication, and Measurement*, Artech House, Norwood, MA, USA, 2014.
6. Ghorbani, H., A. Tavakoli, M. Rabbani, and P. Dehkhoda, "Dualpolarized reflectaray element using open-loop patches," *Proc. IEEE Int. Symp. Antennas Propag. USNC/URSI Nat. Radio Sci. Meeting*, 2179–2180, Vancouver, BC, Canada, Jul. 2015.
7. Costanzo, S., et al., "Dual-band dual-linear polarization reflectarray for mmWaves/5G applications," *IEEE Access*, Vol. 8, 78183–78192, 2020.
8. Gao, S., Q. Luo, and F. Zhu, *Circularly Polarized Antennas*, Wiley, Hoboken, NJ, USA, 2013.
9. Liao, T., et al., "Broadband circular polarized reflectarray based on multi-resonance unit," *International Journal of RF and Microwave Computer-Aided Engineering*, Vol. 31, No. 6, e22618, 2021.
10. Naseri, P., et al., "A dual-band dual-circularly polarized reflectarray for K/Ka-band space applications," *IEEE Transactions on Antennas and Propagation*, Vol. 68, No. 6, 4627–4637, 2020.
11. Yu, A., F. Yang, A. Z. Elsherbeni, J. Huang, and Y. Kim, "An offset-fed X-band reflectarray antenna using a modified element rotation technique," *IEEE Transactions on Antennas and Propagation*, Vol. 60, No. 3, 1619–1624, Mar. 2012.
12. Strassner, B., C. Han, and K. Chang, "Circularly polarized reflectarray with microstrip ring elements having variable rotation angles," *IEEE Transactions on Antennas and Propagation*, Vol. 52, No. 4, 1122–1125, Apr. 2004.
13. Wu, G. B., S. W. Qu, S. Yang, and C. H. Chan, "Broadband, single-layer dual circularly polarized reflectarrays with linearly polarized feed," *IEEE Transactions on Antennas and Propagation*, Vol. 64, No. 10, 4235–4241, 2016.
14. Abadi, S. M. A. M. H. and N. Behdad, "Broadband true-time-delay circularly polarized reflectarray with linearly polarized feed," *IEEE Transactions on Antennas and Propagation*, Vol. 64, No. 11, 4891–4896, 2016.
15. Li, Y., M. E. Bialkowski, and A. M. Abbosh, "Single layer reflectarray with circular rings and open-circuited stubs for wideband operation," *IEEE Transactions on Antennas and Propagation*, Vol. 60, No. 9, 4183–4189, Sep. 2012.
16. Farias, R. L., C. Peixeiro, and M. V. T. Heckler, "Single layer dual-band dual-circularly polarized reflectarray for space communications," *IEEE Transactions on Antennas and Propagation*, Vol. 70, No. 7, 5989–5994, 2022.

17. Zhou, Q., L. Guo, and W. Feng, "A single-layered wideband circularly polarized reflectarray using a linearly polarized feed," *Microwave and Optical Technology Letters*, 2022.
18. Visser, H. J., *Array and Phased Array Antenna Basics*, John Wiley & Sons, Hoboken, NJ, USA, 2006.
19. Bhattacharyya, A. K., "Phased array antennas," *Floquet Analysis, Synthesis, BFNs, and Active Array Systems*, John Wiley & Sons Inc. Publication, Hoboken, NJ, USA, 2006.
20. James, J. R., *Handbook of Microstrip Antennas*, Vol. 1, IET, 1989.